

AN IMPROVED CONTROL SYSTEM FOR VAN DE GRAAFF ACCELERATORS

by

E. A. Gere, H. P. Lie and G. L. Miller  
Bell Telephone Laboratories, Incorporated  
Murray Hill, New Jersey

Summary

In an effort to improve the energy stability and operating convenience of the Rutgers-Bell FN Tandem, a study has been made of the processes involved in the standard Van de Graaff corona stabilization system. In the light of these observations, a terminal voltage control system has been designed using error signals derived both from the slit system and the capacity pickoff plates.

The system operates using either the standard slit system, or the machines' Generating Voltmeter as the terminal voltage reference, switching automatically to the G.V. system when beam is lost for any reason.

Introduction

The usual control loop of a shunt regulated Van de Graaff is shown in Fig. 1.

Excluding complicating factors, the operation is as follows; a change in terminal potential changes the momentum of the beam, which results in a change in the angle of deflection through the magnet, and a lateral displacement of the beam position at the reference slits (only one of which is shown for clarity). The resulting change in the beam current on the slit produces an error voltage which, when applied to the corona tube causes a change in the field emission of the corona points. The field emitted electrons are rapidly captured on CO<sub>2</sub> molecules in the high pressure tank gas, and drift as negative ions to the terminal, thus closing the loop.

Factors Influencing Terminal Stability

The phenomena which limit the machines' ultimate energy stability may be categorized as two types: (1) the sources of terminal voltage variations, and (2) the characteristics of the control loop which limit the gain available to reduce the terminal variations. Space limitations permit only a cursory description of the effects investigated.

Sources of Terminal Voltage Fluctuation

Investigation of terminal voltage fluctuation included the following.

Corona Current Fluctuation. A constant current configuration was tested which reduced the corona current noise but the resulting increase in the dynamic impedance of the corona adversely affected its natural regulating effect for slow terminal voltage variations.

Belt Charging Current Fluctuation. The most serious variation in the belt charging current, which is the largest source of terminal voltage variation, occurs at the period of rotation of the belt (~0.4 s). Measurements of the charging supply current, (which is not constant for frequencies >1c/s), and terminal voltage ripple revealed that the result of making the charge deposited on the belt constant over all frequencies would be to decrease the terminal ripple by only ~25%. The use of a belt which charges uniformly is a most effective way to gain energy stability.

Radiation Induced Currents. These currents, which flow through the gas to the tank wall, have a noise component, of which the most noticeable effect is a spurious signal on the capacitive pickoff plates which becomes serious at low frequencies.

Control Loop Characteristics

The two features of the system which make it recalcitrant from the point of view of good closed-loop behavior are the ion-transit time from the corona to the terminal, and the response of the slit system to beam motion.

Ion Transit Time. A measurement was made of the response of the terminal to a burst of charge from the corona. The results, which are shown in Fig. 2, are at variance with previous measurements. Considering that the terminal is largely capacitive, one sees that the burst of charge produces a nearly constant displacement current for a transit time of ~30 ms. (It is this transit time which is responsible for the loop oscillation frequency of ~30 c/s in FN machines.)

Corona Transfer Function. To a first approximation the terminal can be approximated by a lumped time constant  $T_2 = C_T R_T$  as shown in Fig. 1. Here the shunt terminal resistance  $R_T$  comprises the column resistance of parallel with the corona impedance, while  $C_T$  is ~100 pf. It can then be shown that the voltage-voltage transfer function from the grid of the corona tube to the terminal is given by

$$\frac{L\{V_T(t)\}}{L\{V_G(t)\}} = \frac{R_T(1-e^{-pT_1})}{p(1+pT_2)} \quad (1)$$

where  $V_T(t)$  is the terminal potential,  $V_G(t)$  is the grid potential and  $L$  is the Laplace transform operator. The ion transit time  $T_1$  is substantially independent of terminal potential (this is because the corona points are moved as the terminal potential is changed.)

Slit System. Two features of the slit response are of concern. The first, termed "geometrical phase advance", is that the output of the slit system is not linearly related to beam position, and produces disproportionately large signals for large beam excursions.

The second difficulty arises from the use of diodes as loads at the slits to make the slit system output a function of beam position rather than beam intensity, for small excursions. The problem here is that this introduces a variable phase lag of time constant  $T_L = C_S R_{TN}$ , where  $R_{TN}$  is the diode impedance at the operating slit current (e.g.  $R_{TN} = 30 \text{ M}\Omega$  at 1 na,  $C_S \sim 100 \text{ pf}$  therefore  $T_L \sim 3 \text{ ms}$  increasing to 30 ms at 0.1 na etc.). These two factors render the slit system a poorly behaved feedback element, although both problems disappear if fast feedback is derived from some other source, for in that case the slit signal can be rolled off at some appropriate frequency to nullify all such effects. This is the course followed in the present design as indicated in the next section.

#### The New Control System

A block diagram of the new control system is shown in Fig. 3. The major points of the rationale of the design follow from the remarks of the previous section. Slow feedback is derived from the slits and fast feedback from the output of an integrator ( $T = 1 \text{ sec}$ ) connected to the capacity pick-off plates. The crossover frequency between fast and slow signals is defined by  $C_2$  times the parallel equivalent resistance of  $R_2$  and  $R_3$ , and is set at  $\sim 70 \text{ ms}$ . Since it can be shown that the deleterious effects of the transfer function of equation (1) can be compensated to first order by a phase advance, such a network is added, comprising  $R_4$ ,  $R_5$ ,  $C_3$ .

In addition, a new slit preamplifier, shown in Fig. 4, was designed. This uses dual emitter transistor  $Q_4$  to generate a signal of the form  $(I_1 - I_2) / (I_1 + I_2)$ , where  $I_1$ ,  $I_2$  are the slit currents, in a manner that is closely analogous to that of Ref. 2. The nearly identical emitter diodes provide good input balance for currents as small as  $10^{-11}$  amps. In addition, though this is not vitally important because of the choice of crossover frequency, the input impedance at both inputs is always lower than that of a single diode carrying the same slit current.

The new configuration also provides an independent output proportional to the log of the slit current. This is used to drive a discriminator, shown in Fig. 3, which produces a push-pull output signal. Field effect transistors  $Q_1$ ,  $Q_2$ , in Fig. 3, are operated by this discriminator in such a way that if beam is present at the slit,  $Q_2$  opens and  $Q_1$  closes so as to transfer control to the generating voltmeter. In this way the lock-in range of the machine spans its entire operating energy range.

An additional feature provided in the design is that when the machine is under slit control it is possible, if desired, to operate in a mode in

which the balance of the generating voltmeter is constantly readjusted to indicate changes in terminal potential. As soon as beam is lost, however, the self-balancing feature is automatically switched off for the duration of the time the machine is under G.V. control. On regaining the beam it is switched back on, and so on.

Crucial to the present design is the question of whether it is valid to employ the capacity pickoff signal for fast feedback. This was answered affirmatively by noting that the terminal voltage and slit preamplifier output voltage track one another at high frequencies, and for small excursions as indicated by Fig. 5. From this it follows that they are capable of providing substantially the same information and hence that the mixed feedback scheme is a viable one, provided that the crossover frequency is sufficiently high that the spurious response of the pickoff plates to currents in the gas is well attenuated. The crossover frequency of the present design was chosen with this in mind.

One additional feature of convenience is that the output of the capacity pickoff plate integrator is displayed on an oscilloscope at all times, acting as a monitor of terminal voltage ripple. Its sensitivity is  $0.1 \text{ volts } \text{kV}^{-1}$ .

#### The Generating Voltmeter

As originally constructed and installed, the generating voltmeter exhibited a nonlinearity of  $\sim 1\% \text{ MV}^{-1}$ . In order to improve this performance three steps were taken: first the location of the unit was moved from its original position, right next to the corona points, to a port almost diametrically opposed to the corona points, second the aluminum stator and rotor plates were polished and gold plated; and finally the insulating plate supporting the stator plates was replaced by a metal one with hidden insulators to prevent local charge buildup with consequent field distortion.

Following these modifications the voltmeter linearity was greatly improved, although it is not known which change was the most significant one in producing this result.

An improved electronic system was also developed to provide the facility of controlling the terminal potential from the generating voltmeter. This is useful in the absence of beam falling on the control slits, as when bringing the machine up to energy, or in the case of temporary loss of beam when operating, etc.

The principle employed is shown in Fig. 6, and depends on the observation that each time the generating voltmeter windmill rotates one quarter of a turn a quantity of charge  $V_T C_0$  ( $\sim 10^{-8}$  Coulombs  $\text{MV}^{-1}$ ) flows to the uncovered stator plates and this quantity of charge is independent of rotor speed. It is clear that if a means can be found to compare this charge with a stable reference charge, for instance by subtraction and integration of their difference, a suitable control signal would be available.

These functions are performed by the system of Fig. 6 which employs a technique which has been named negative feedback to distinguish it from negative feedback. As can be seen from the diagram, if a signal current flows into or out of the summing point of amplifier  $A_1$  all that current must be supplied by either  $Q_1$  or  $Q_2$ . If one assumes sufficiently high  $\beta$ 's in  $Q_1$  and  $Q_2$ , (e.g. each can be a Darlington pair or alternatively field effect transistors can be used) substantially all of the input current is made available at the  $Q_1$ ,  $Q_2$  collectors, i.e. the input current can be made to flow into an external circuit. In this way the negative current excursions from the generating voltmeter plates are caused to flow through  $Q_1$ , hence into the operational integrator  $A_3$ ,  $C_4$ , while the positive excursions flow through  $Q_2$  to a meter which indicates the terminal voltage in the usual way. The presence of the capacitor  $C_1$  ( $\sim 1 \mu\text{f}$ ) is important because it guarantees exact equality in the magnitude of the total charge that flows through  $Q_1$  and  $Q_2$ .

Each time the G.V. rotor moves one quarter turn the output of  $A_1$  moves up or down (the signal at this point is a square wave) and hence fires the charge pump comprising  $Q_4$ ,  $R_1$  and  $C_3$ . The resulting charge flowing through  $C_3$  is routed back into the  $A_3$ ,  $C_4$  integrator via a second negative feedback loop around  $A_2$  in such a way as to provide the desired reference charge subtraction. The potentiometer  $R_1$  is a motor drive which can be connected to the error signal output, thus turning the unit into a self-balancing potential (independent of G.V. rotor speed).

#### Performance

Comparison of the above system with a standard system using slit feedback reveals three areas of improvement. Use of the capacity pickoff for the fast feedback signal results in reduction terminal fluctuations by about a factor of three. The phase advance network results in relatively little improvement as seen from the

capacity pickoff scope, but has the effect of reducing lower frequency fluctuations, and hence reduces the intensity fluctuations of the beam considerably in many situations. With a "healthy" machine, the terminal voltage fluctuations are almost entirely within a 600 V envelope. The use of the dual-emitter transistor in the slit preamp has improved the input balance at very low currents, making it possible to operate with slit currents on the order of  $10^{-11}$  A.

The performance of the generating voltmeter can be judged from Fig. 7. This linearity curve was obtained by measuring the terminal voltage, with the machine under slit control, for 5 charge states of oxygen while holding the analyzing magnet field constant.

Other important performance parameters of the system are a long term stability of  $\pm 2$  kv and a shift in reading due to corona current changes of  $\sim 30$  volts per microampere.

#### Conclusion

The above system has resulted in an improvement in terminal voltage stability and operating convenience. The generating voltmeter control is sufficiently stable to be used as the only reference in many experiments, such as those in which several projectile charge states might be used simultaneously. Because of the corona transit time delay, it appears difficult to raise the gain of the control loop by any significant factor over that of the present system by use of compensating networks.

#### References

1. A. J. Gale, Accelerator Design Concepts, Nuc. Instr. and Meth., 28, No. 1, pp. 1-9 (1964).
2. E. A. Gere and G. L. Miller, A High Speed Analog Pulse Divider, IEEE Trans. on Nuc. Sci., NS-11, No. 4, pp. 382-387 (1964).

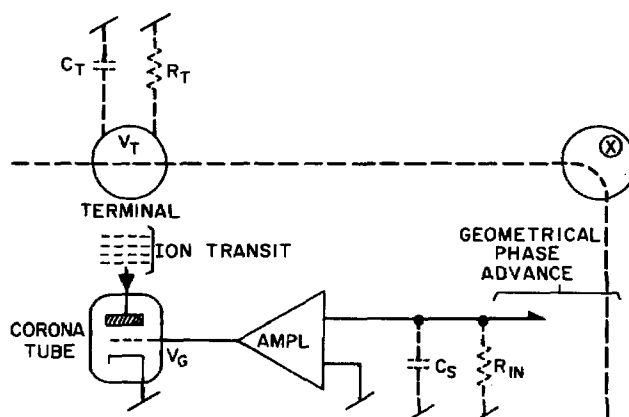


Fig. 1. Standard corona regulated Van de Graaff control loop.

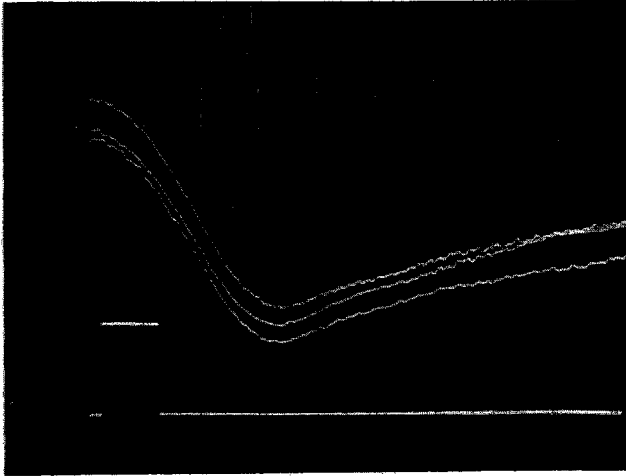


Fig. 2. Response of the terminal potential to a pulse at the grid of the corona tube. Upper trace: Terminal voltage measured by capacitive pickoff. Scale: 5 kV/div. Lower trace: Pulse on grid of corona tube. Scale: 25 V/div. Horiz. scale: 10 ms/div.

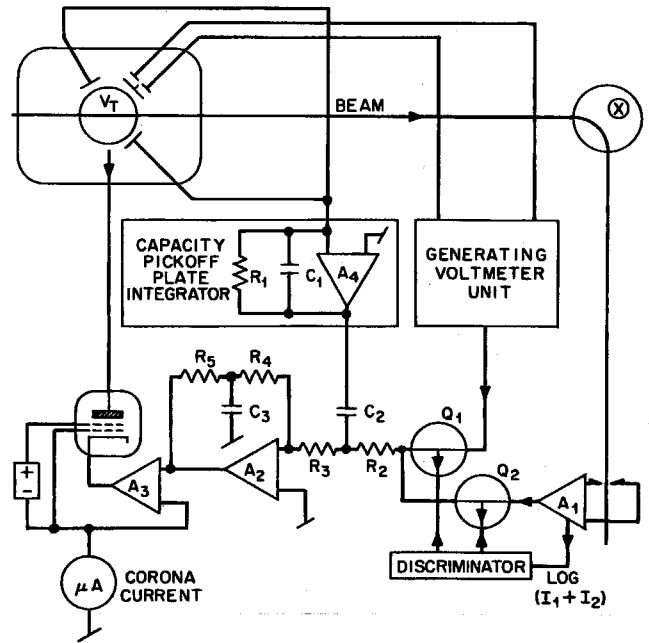


Fig. 3. Improved control system block diagram.

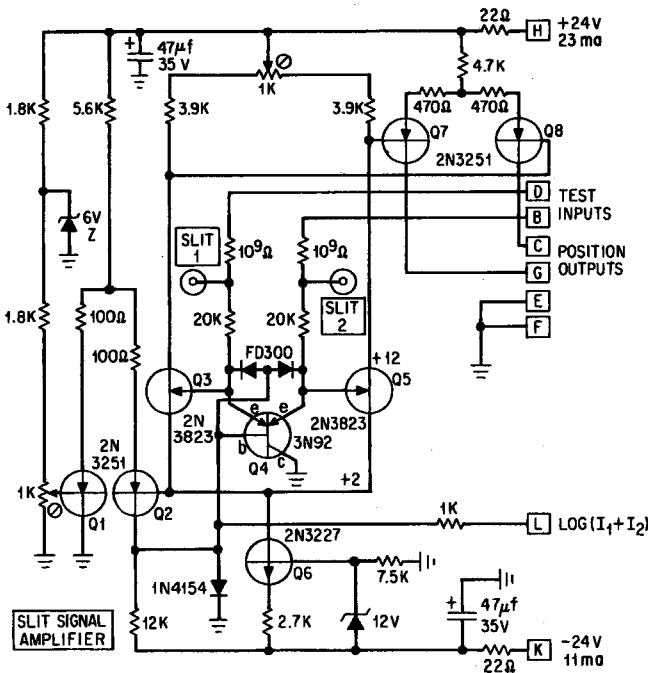


Fig. 4. Slit signal preamplifier schematic.

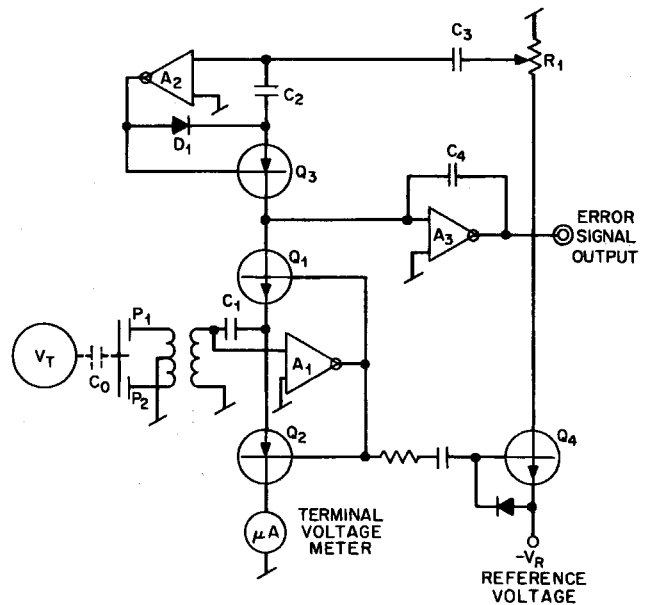


Fig. 5. Generating volt meter electronic block diagram.

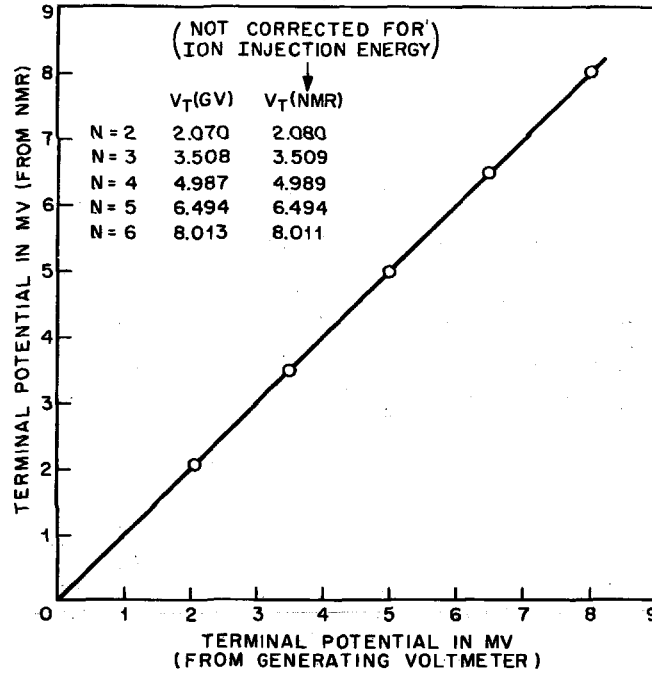


Fig. 7. Generating voltmeter system linearity.

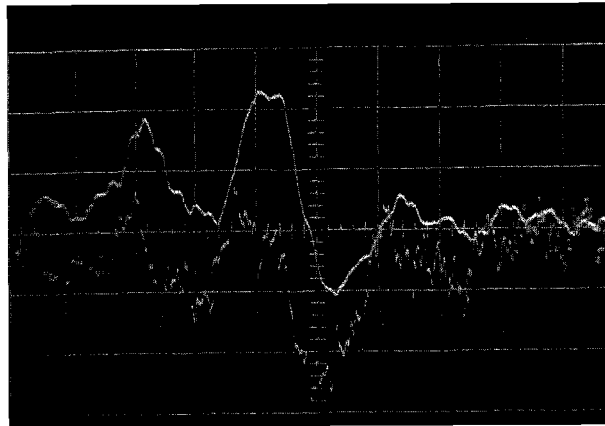


Fig. 6. Comparison of slit preamplifier signal (top) and capacity pickoff integrator signal (bottom) showing phase lag of the slit signal, and deviation of capacitive pickoff signal at low frequencies. Vert. scale: 500 V/div. terminal voltage equivalent. Horiz. scale: 100 ms/div.